

# Structural and electronic properties of [0001] AlN nanowires: A first-principles study

Yelong Wu,<sup>1,a)</sup> Guangde Chen,<sup>1</sup> Honggang Ye,<sup>1</sup> Youzhang Zhu,<sup>1</sup> and Su-Huai Wei<sup>2</sup>

<sup>1</sup>Department of Applied Physics, Xi'an Jiaotong University, Xi'an 710049, People's Republic of China

<sup>2</sup>National Renewable Energy Laboratory, Golden, Colorado 80401, USA

(Received 27 August 2008; accepted 2 September 2008; published online 28 October 2008)

Using first-principles methods, we investigated the atomic relaxations, electronic structure, and formation energies of nonpassivated AlN nanowires along [0001] directions. We find that all the nanowires prefer to have (10 $\bar{1}$ 0) lateral facets and all the wires with (10 $\bar{1}$ 0) lateral facets are semiconductors with a direct band gap. However, surface states that arise from the facet atoms exist inside the bulklike band gap, which can have a large effect on the optoelectronic properties of the nanowires. Our calculated formation energies of the nanowires show that there is a sublinear relationship between the formation energy and surface-to-volume ratio, indicating that the surface effect is localized and becomes more important for small nanowires. © 2008 American Institute of Physics. [DOI: 10.1063/1.3003528]

## I. INTRODUCTION

Nanostructures of semiconducting materials are currently attracting a lot of interest as they are expected to play an important role in the development of future nanoscale technologies. Nanowires are one-dimensional nanostructures with electrical carriers confined in the other two (perpendicular) directions. They have numerous potential applications in science and technology, such as optoelectronic devices, nanoswitches, and nanocontacts,<sup>1–3</sup> due to their low dimensionality and unique fascinating properties that are noticeably different from those of quantum dots and bulk. AlN nanowires appear to be an especially appealing choice. AlN material has large band gap of  $\sim 6.0$  eV, low electron affinity,<sup>4–6</sup> and other peculiar features that make it a promising candidate for field electron emitter, scanning probes, flexible pulse wave sensors, nanomechanical resonators, and light-emitting diodes.

Recently, randomly oriented<sup>7,8</sup> and aligned<sup>9</sup> AlN nanowires have been fabricated by different methods. Our research group also has synthesized hexagonal single crystal *h*-AlN nanowires through the direct reaction of anhydrous AlCl<sub>3</sub> with NaN<sub>3</sub> at a low temperature of 450 °C for about 24 h.<sup>10</sup> This is a simple method to synthesize hexagonal single crystal *h*-AlN nanowires, which has better morphology than the nanometer AlN whiskers produced by Wu. *et al.*<sup>11</sup> in 2004. In our experiments, about 70%–80% of the products are long straight wires and have nonbranched morphology. The relatively uniformed *h*-AlN single crystal nanowires range in diameters from 40 to 60 nm and most wires are as long as several micrometers. According to the results of electron diffraction and x-ray diffraction, the AlN nanowires grow along the [0001] direction. However, despite the progress in the preparation of such nanowires, relatively little is known about the basic physical properties of AlN nanowires. Few theoretical investigations have been performed

on the nanowires,<sup>12,13</sup> mainly focusing on AlN nanotubes. A deeper understanding of the structural and electronic properties of AlN nanowires is still lacking. Hence, in order to guide future experiments and fully exploit these materials for innovative nanodevice applications, the structural and electronic properties of these nanostructures need to be investigated in more detail.

In this letter, we investigate the atomic relaxations, electronic structures, and formation energies of nonpassivated AlN nanowires oriented along [0001] with hexagonal cross section enclosed by (10 $\bar{1}$ 0) facets from first-principles. We find that for these nonpassivated nanowires the surface states, which appear in band gap play an important role. We also show that there exists a linear correlation between the formation energy and surface-to-volume ratio.

## II. COMPUTATIONAL METHODS

In our work, all the structural optimizations and energy calculations are performed by using the density-functional theory in the generalized-gradient approximation.<sup>14</sup> The projected augmented wave method<sup>15</sup> as implemented in Vienna *ab initio* simulation package<sup>16,17</sup> was employed to investigate nanowires diameters from 3.6 to 15.7 Å. Figure 1 shows the structures of the nanowires that we calculated. In addition, structural properties of nonpolar (10 $\bar{1}$ 0) surfaces have been calculated, which will serve as a reference when presenting our results for the nanowires. The energy cutoff was set at 500 eV throughout the calculations. To eliminate the interaction between neighboring nanowires, we choose vacuum regions of  $3a$  (lattice constant) in the two orthogonal directions of *x-y* plane. For the surface and nanowire calculations, we used our optimized lattice parameters for bulk AlN:  $a = 3.129$  Å,  $c = 5.012$  Å, and  $u = 0.381$ , which are very close to the experimental values,  $a = 3.112$  Å and  $c = 4.982$  Å.<sup>18</sup> A  $9 \times 9 \times 5$  *k*-point mesh is used to test bulk AlN properties, and a  $2 \times 2 \times 5$  mesh is used for the nanowires. The atomic

<sup>a)</sup>Electronic mail: wuyelong520@gmail.com.

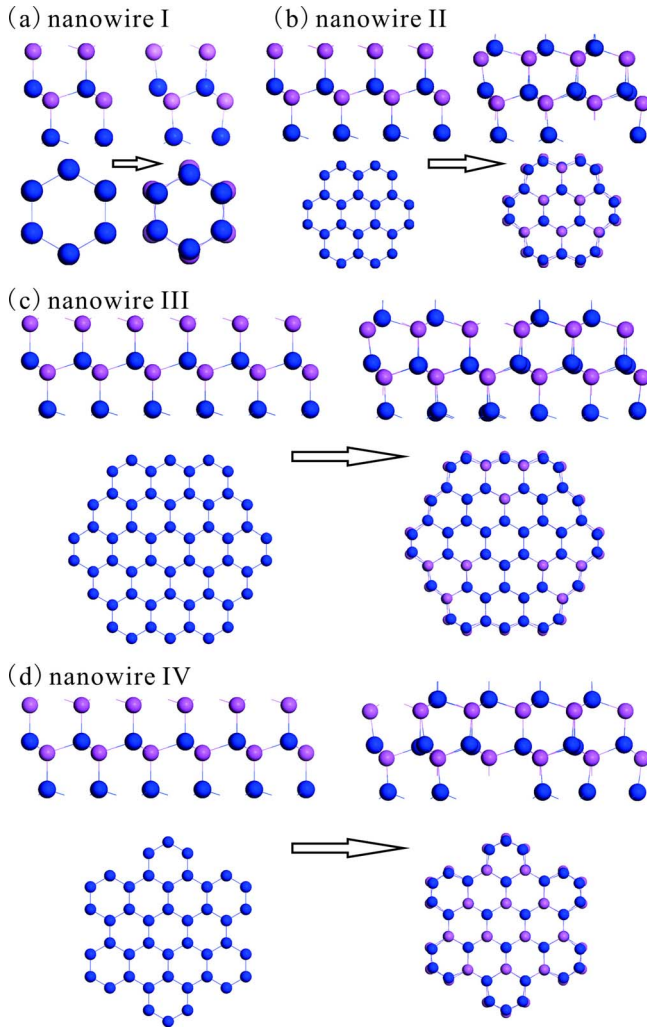


FIG. 1. (Color online) Side and top views of initial (left) and optimized (right) AlN nanowires. Red (gray) and blue (dark) spheres represent N and Al atoms, respectively.

positions have been relaxed until the maximum force was smaller than  $0.03 \text{ eV}/\text{\AA}$ .

### III. RESULTS AND DISCUSSION

We first relaxed the nonpolar AlN  $(10\bar{1}0)$  and  $(11\bar{2}0)$  surfaces, which were modeled using periodic slabs with ten

TABLE I. Structural properties of the optimized AlN nanowires with  $(10\bar{1}0)$  surface.

Structures	Nanowire I	Nanowire II	Nanowire III	$(10\bar{1}0)$
$d_{N_1-Al_1}$ ( $\text{\AA}$ )	1.8017	1.7701	1.7668	1.7600
$d_{Al_1-N_2}$ ( $\text{\AA}$ )		0.7139	0.7390	0.7527
$d_{N_2-Al_2}$ ( $\text{\AA}$ )		1.9171	1.7668	1.9135
$\Delta_{N_1-Al_1}$ ( $\text{\AA}$ )	0.2148	0.2188	0.2010	0.2112
$\Delta_{Al_1-N_2}$ ( $\text{\AA}$ )		0.8914	1.1149	0.6348
$\Delta_{N_2-N_3}$ ( $\text{\AA}$ )		1.8481	1.7609	1.8179
$\Delta_{Al_2-N_2}$ ( $\text{\AA}$ )		0.0751	0.0664	0.0740
$\Delta_{N_3-Al_3}$ ( $\text{\AA}$ )		0.0341	0.0300	0.0366
$\omega$ (deg)	6.798	8.193	8.179	6.843
$d_{\text{surf}}$ ( $\text{\AA}$ )	1.841	1.854	1.857	1.862
$d_{\text{inter}}$ ( $\text{\AA}$ )		1.933	1.918	1.911
$d_{\text{all}}$ ( $\text{\AA}$ )		1.876	1.887	1.911

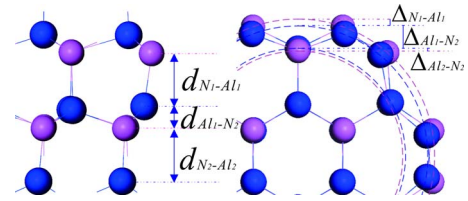


FIG. 2. (Color online) Side (left) and top (right) views of nanowire II. Red (gray) and blue (dark) spheres represent N and Al atoms, respectively.  $d_{A-B}$  and  $\Delta_{A-B}$  represent the distance between  $A$  atoms layer and  $B$  atoms layer in the directions perpendicular and parallel to the surface, respectively.

AlN bilayers separated by  $10 \text{ \AA}$  vacuum region and found that the surface energies are  $0.135$  and  $0.140 \text{ eV}/\text{\AA}^2$ , respectively. We attribute this energetic advantage of AlN  $(10\bar{1}0)$  surface to the lower density of dangling bonds, which is  $0.128/\text{\AA}^2$  as compared with  $0.147/\text{\AA}^2$  of AlN  $(11\bar{2}0)$  surface. Then, we have explored two competing geometries with similar diameters but different lateral facets,  $(10\bar{1}0)$  and  $(11\bar{2}0)$ , respectively, as shown in Figs. 1(c) and 1(d). The surface energies of the AlN nanowire with  $(10\bar{1}0)$  is  $0.143 \text{ eV}/\text{\AA}^2$ , while that of the  $(11\bar{2}0)$  faceted one is  $0.153 \text{ eV}/\text{\AA}^2$ , namely, the former is found to be energetically more favorable than the latter. The difference between nanowires and surfaces stems from the lower coordination of facet atoms. As a result of the discussions mentioned above, it is the  $(10\bar{1}0)$  surfaces that are the preferable lateral facets of AlN nanowires rather than  $(11\bar{2}0)$  surfaces, which agree with the results of Zhao *et al.*<sup>12</sup> We thus focus on AlN nanowires with  $(10\bar{1}0)$  facets in our work.

The relaxed atomic configurations of  $(10\bar{1}0)$  surface and our AlN nanowires are given in Table I, in which  $d_{A-B}$  and  $\Delta_{A-B}$  represent the distance between  $A$  atom layer and  $B$  atom layer in the directions perpendicular and parallel to the surface, respectively (Fig. 2). First, we discuss the relaxed result of  $(10\bar{1}0)$  surface. The bond length of the AlN dimers on the surface is  $1.773 \text{ \AA}$ , which corresponds to a 7% contraction with respect to the bond length calculated for bulk ( $1.911 \text{ \AA}$ ). The vertical displacement between N and Al at-

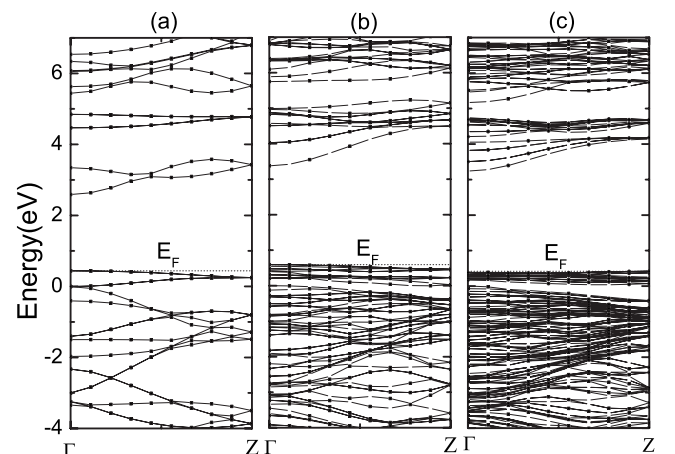


FIG. 3. Band structure diagrams (a) nanowire I, (b) nanowire II, and (c) nanowire III. The energy zero is taken arbitrarily to be the VBM of the bulklike states.

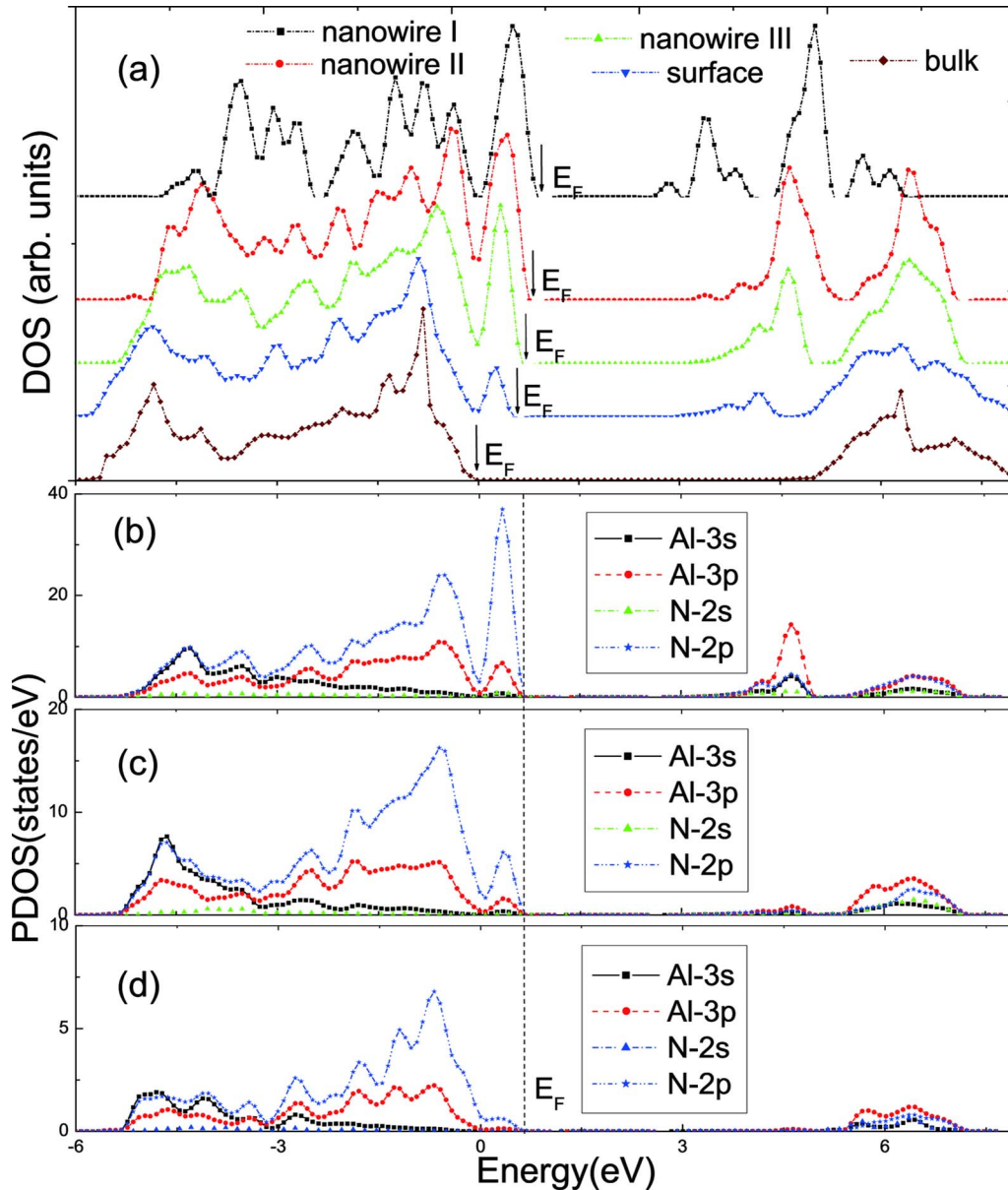


FIG. 4. (Color online) (a) Total DOS for bulk AlN, surface, nanowires I, II, and III. [(b)–(d)] PDOS of nanowire III: (b) outermost bilayer atoms, (c) secondary bilayer atoms, and (d) core atoms. The energy zero is taken arbitrarily to be the VBM.

oms located in the first layer is  $0.211 \text{ \AA}$  and corresponds to a buckling angle of  $6.8^\circ$ , as both N and Al atoms relax toward to the bulk region but not by the same amount. The Al atom moves  $0.24 \text{ \AA}$  from its bulk position, while N remains close to its original position, relaxes only  $0.03 \text{ \AA}$ . In fact, this phenomenon has also been found in recent first-principles calculations for ZnO.<sup>19</sup>

All the relaxation results of the AlN nanowires are listed in Table I and Fig. 1 shows the initial and relaxed structures with both side and top views. The obvious difference between the optimized and initial structures is that the in-plan Al–N on the surface are no longer on the same plan after the relaxation due to the buckling of the Al–N atoms, which is similar to the result found for the  $(10\bar{1}0)$  surface. The buckling angle of the outermost Al–N dimer is  $6.80^\circ$ ,  $8.19^\circ$ , and  $8.18^\circ$  for nanowires I, II, and III, respectively. The bond angles around the Al atom on the out most layers become

$114.9^\circ$ ,  $114.9^\circ$ , and  $115.7^\circ$  for nanowire I,  $113.5^\circ$ ,  $113.5^\circ$ , and  $117.2^\circ$  for nanowire II, and  $115.8^\circ$ ,  $115.8^\circ$ , and  $117.3^\circ$  for nanowire III, thus the Al atom relaxes toward a  $sp^2$  configuration while the N atom moves closer to the  $p^3$  configuration with bond angles of  $108.2^\circ$ ,  $108.2^\circ$ , and  $96.5^\circ$  for nanowire I,  $108.0^\circ$ ,  $108.0^\circ$ , and  $105.1^\circ$  for nanowire II, and  $105.9^\circ$ ,  $105.9^\circ$ , and  $116.9^\circ$  for nanowire III. The comparison of the average Al–N bond lengths of  $d_{\text{surf}}$  and  $d_{\text{inter}}$ , as Table I shows, is understandable that surface atoms have a shorter average Al–N bond length due to reduced coordination numbers. It can be also found that the average Al–N bond lengths of all the atoms  $d_{\text{all}}$  shortens along with the decrease in the diameter of nanowire or increase in the surface-to-volume ratio. This reduction in the Al–N bond length with decreasing diameter of the nanowire,<sup>20</sup> combined with quantum confinement effect, could lead to an anomalous blueshift of the cathodoluminescence (CL) emission as found in ZnO.<sup>21</sup>

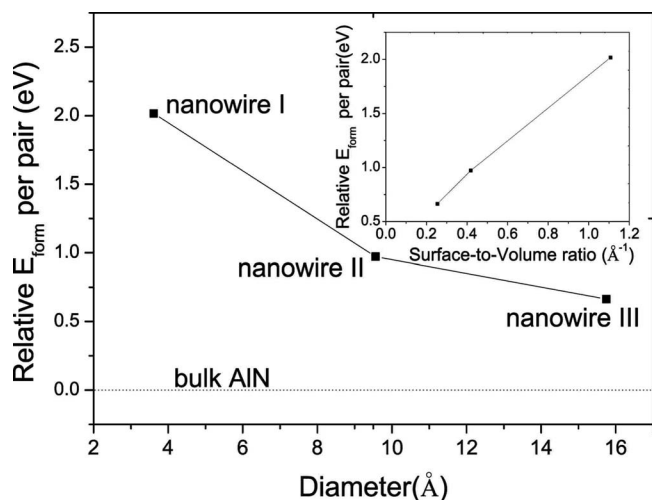


FIG. 5. Relative  $E_{\text{form}}$  per pair of the optimized nanowires as a function of the diameter. The inset shows the relative  $E_{\text{form}}$  per pair of the optimized nanowires as a function of the surface-to-volume ratio. The energy zero is taken arbitrarily to be the formation enthalpy of bulk AlN.

Figure 3 shows the band structures of the AlN nanowires corresponding to the configurations shown in Figs. 1(a)–1(c). The total densities of states (DOSs) of the nanowires as well as bulk and the (10 $\bar{1}$ 0) surface are presented in Fig. 4(a). To obtain more details about the electronic structure of the optimized nanowire, we also show the projected DOSs (PDOSs) of nanowire III, which is a typical representation of the nanowires, in Figs. 4(b)–4(d).

The band structures and DOS indicate that (1) all these AlN nanowires with nonpolar surfaces have a semiconducting character and a direct band gap at the  $\Gamma$  point. (2) There are significant amounts of occupied surface states close to the valence band maximum (VBM) and unoccupied states below the conduction band minimum (CBM). This phenomenon is quite different from ZnO nanowires, where surface states lay just below the VBM or above the CBM.<sup>21</sup> (3) As a whole, the shapes of the DOS are similar for the three nanowires, but due to quantum confinement effects, the band gap of the bulklike states increases in energy when the size of the nanowire decreases, whereas the bandwidth of the surface-like states increases when the wire size decreases. (4) The occupied surface bands are mostly formed by N  $2p$  orbitals, whereas the unoccupied surface bands consists mostly of Al  $3s$  and  $3p$  orbitals.

Finally, we studied the relative stability of structures as a function of the wire size by calculating the formation energies of the nanowires. The formation energy (per pair) is defined with respect to the chemical potentials of the constituents, written by

$$E_{\text{form}} = (E_{\text{tot}}[n\text{AlN}] - n\mu_{\text{Al}} - n\mu_{\text{N}})/n,$$

where  $n$  is the number of AlN pairs,  $\mu_{\text{Al}}$  and  $\mu_{\text{N}}$  are the chemical potentials of Al and N obtained from face-centered cubic metal Al and isolated N<sub>2</sub> molecule, respectively,  $E_{\text{tot}}[n\text{AlN}]$  is the calculated total energy of the nanowire. Figure 5 shows the relative  $E_{\text{form}}$  per pair of the optimized nanowires as a function of the diameter and surface-to-

volume ratio, respectively. It is obvious that the formation energy decreases with increasing diameters, approaching the corresponding bulk value. The relationship between the formation energy and surface-to-volume ratio is nearly linear, indicating that surface effects play a dominant role in these small size nanowires.

#### IV. CONCLUSIONS

In summary, we have performed first-principles calculations on [0001] oriented AlN nanowires with different diameters. The study finds that the (10 $\bar{1}$ 0) surface is the preferable lateral facets of the AlN nanowires. We find that all the nanowires are semiconductors. However, surface states that arise from the facet atoms exist inside the bulklike band gap. This is quite different from that for the more ionic ZnO, in which no surface state is found in the gap of ZnO nanowires with similar nanowire structure. Our calculated formation energies of the nanowires show that there is a sublinear relationship between the formation energy and surface-to-volume ratio, indicating that the surface effect is localized and becomes more important for small nanowires.

#### ACKNOWLEDGMENTS

We gratefully acknowledge the financial support of China National Natural Science Fund (Grant No. 10474078) and the computing support of the “Digital Information Process and Calculation Laboratory” of Xi’an Jiaotong University. The work at NREL is supported by the U.S. DOE under Contract No. DE-AC36-99GO10337.

- <sup>1</sup>D. Appell, *Nature (London)* **419**, 553 (2002).
- <sup>2</sup>A. M. Morales and C. M. Lieber, *Science* **279**, 208 (1998).
- <sup>3</sup>C. M. Lieber, *Nano Lett.* **2**, 81 (2002).
- <sup>4</sup>I. Vurgaftman, J. R. Meyer, and L. R. Ram-Mohan, *J. Appl. Phys.* **89**, 5815 (2001).
- <sup>5</sup>S. P. Grabowski, M. Schneider, H. Nienhaus, W. Monch, R. Dimitrov, O. Ambacher, and M. Stutzmann, *Appl. Phys. Lett.* **78**, 2503 (2001).
- <sup>6</sup>J. Li, K. B. Nam, M. L. Nakarmi, J. Y. Lin, H. X. Jiang, P. Carrier, and S.-H. Wei, *Appl. Phys. Lett.* **83**, 5163 (2003).
- <sup>7</sup>C. K. Xu, L. Xue, C. R. Yin, and G. H. Wang, *Phys. Status Solidi A* **198**, 329 (2003).
- <sup>8</sup>Q. Wu, Z. Hu, X. Z. Wang, Y. N. Lu, K. F. Huo, S. Z. Deng, N. S. Xu, B. Shen, R. Zhang, and Y. Chen, *J. Mater. Chem.* **13**, 2024 (2003).
- <sup>9</sup>Q. Wu, Z. Hu, X. Z. Wang, Y. M. Hu, Y. J. Tian, and Y. Chen, *Diamond Relat. Mater.* **13**, 38 (2004).
- <sup>10</sup>H. M. Lv, G. D. Chen, H. G. Ye, and G. J. Yan, *J. Appl. Phys.* **101**, 053526 (2007).
- <sup>11</sup>C. Z. Wu, Q. Yang, C. Huang, D. Wang, P. Yin, T. W. Li, and X. Yi, *J. Solid State Chem.* **177**, 3522 (2004).
- <sup>12</sup>M. W. Zhao, Y. Y. Xia, X. D. Liu, Z. Y. Tan, B. D. Huang, C. Song, and L. M. Mei, *J. Phys. Chem. B* **110**, 8764 (2006).
- <sup>13</sup>S. M. Hou, J. X. Zhang, Z. Y. Shen, X. Y. Zhao, and Z. Q. Xue, *Physica E (Amsterdam)* **27**, 45 (2005).
- <sup>14</sup>J. P. Perdew and Y. Wang, *Phys. Rev. B* **45**, 13244 (1992).
- <sup>15</sup>P. E. Blochl, *Phys. Rev. B* **50**, 17953 (1994).
- <sup>16</sup>G. Kresse and J. Furthmuller, *Comput. Mater. Sci.* **6**, 15 (1996).
- <sup>17</sup>G. Kresse and J. Furthmuller, *Phys. Rev. B* **54**, 11169 (1996).
- <sup>18</sup>I. Vurgaftman and J. R. Meyer, *J. Appl. Phys.* **94**, 3675 (2003).
- <sup>19</sup>W. Fan, H. Xu, A. L. Rosa, T. Frauenheim, and R. Q. Zhang, *Phys. Rev. B* **76**, 073302 (2007).
- <sup>20</sup>M. H. Tsai, Z. F. Jhang, J. Y. Jiang, Y. H. Tang, and L. W. Tu, *Appl. Phys. Lett.* **89**, 203101 (2006).
- <sup>21</sup>C. W. Chen, K. H. Chen, C. H. Shen, A. Ganguly, L. C. Chen, J. J. Wu, H. I. Wen, and W. F. Pong, *Appl. Phys. Lett.* **88**, 241905 (2006).